IEEE Access
Multidisciplinary ⋮ Rapid Review ⋮ Open Access Journal

Received March 15, 2022, accepted April 5, 2022, date of publication April 18, 2022, date of current version April 25, 2022.

Digital Object Identifier 10.1109/ACCESS.2022.3167642

A Node Selection Algorithm Based on Multi-Objective Optimization Under Position Floating

SHENGKAI TIAN[1] **AND ZHENKAI ZHANG**[2]

[1]School of Naval Architecture & Ocean Engineering, Jiangsu University of Science and Technology, Zhenjiang 212100, China
[2]Ocean College, Jiangsu University of Science and Technology, Zhenjiang 212003, China

Corresponding author: Zhenkai Zhang (zhangzhenkai@just.edu.cn)

This work was supported in part by the National Natural Science Foundation of China under Grant 61871203, and in part by the Postgraduate Research & Practice Innovation Program of Jiangsu Province under Grant KYCX21_3501.

ABSTRACT Almost all existing node selection algorithms of the underwater sensor networks (USNs) are designed by assuming ideal environments. However, the position floating of the underwater sensor nodes which caused by ocean currents cannot be ignored in practice. Aiming at solving this problem during underwater target tracking, a node selection algorithm based on multi-objective optimization under position floating was proposed in this paper. First, the error caused by position floating is converted into a floating noise. Then, as the criteria for node selection, both Fisher information matrix (FIM) and mutual information (MI) under position floating are derived by the particle filter under position floating (PF-PF). Finally, the number of nodes, the corresponding FIM and MI are set as the objective function, both nondominated sorting genetic algorithm II (NSGA-II) and Technique for Order of Preference by Similarity to Ideal Solution (TOPSIS) are used to find the optimal node selection scheme. Simulation results show that the proposed algorithm can overcome the influence of position floating, and ultimately, its tracking performance is more stable and accurate.

INDEX TERMS Position floating, node selection, multi-objective optimization, target tracking, underwater sensor networks.

I. INTRODUCTION

Nowadays, as an indispensable part of underwater applications, underwater target tracking has received much attention and research in both the military and civilian fields [1]. In the military field, underwater target tracking can effectively defend the invade of torpedoes, submarines and underwater robots. In the civilian field, it also plays an important role in the protection for marine resources, oil/gas exploration and maritime seismic survey [2].

The commonly used underwater target tracking technologies include target tracking based on traditional acoustic sensor arrays (TASAs), target tracking based on acoustic imaging sensor and target tracking based on underwater sensor networks (USNs) [3]. Target tracking based on TASAs is realized by obtaining the bearing information on target assisted by linear arrays which are pulled by ship. However, TASAs-based technologies may be flawed considering the limited tracking area and poor performance on real time. Although video or image information can be obtained from acoustic imaging sensor-based approaches, their limited sensing range and poor visibility make these approaches not attractive. With the emerging development of wireless sensor networks (WSNs), USNs also has been given extensive attention. With the advantages of flexible distribution, multi dimension, inexpensive equipment and strong concealment, underwater target tracking based on USNs has become a research hotspot in the last decade [4]–[6].

Usually, the underwater sensor nodes in USNs are powered by battery. Limited by the special underwater environment, the battery is un-rechargeable and difficult to replace. Therefore, in USNs, limitation on energy is a common problem. In actual engineering application, this problem is impossible to ignore [7], [8]. Theoretically, the more nodes participate in tracking, the better tracking performance will achieve. However, utilizing all nodes to keep tracking will

The associate editor coordinating the review of this manuscript and approving it for publication was Jonathan Rodriguez.

not only consume too much energy, but will also cause the limited underwater communication bandwidth to be more overwhelmed. Hence, node selection has become an effective way to extend the life of USNs [9]. The reduction in the number of nodes will nonetheless also reduce the tracking performance. Therefore, in practical engineering application, it is worth studying how to effectively balance the number of nodes taken part in tracking and the tracking performance.

At present, many researchers have proposed a number of algorithms to select nodes under different criteria. Huang *et al.* select the node which is closest to the target to participate in target tracking based on Euclidean distance [10]. This algorithm can reduce both energy consumption and communication load significantly. In [11], a local node selection scheme is designed only based on the local information. Then, in [12], only 60% nodes are selected to avoid divergence and achieve more reliable tracking. The authors of [13] select nodes based on the posterior Cramer low bound (PCRLB) and achieve better tracking performance through proper fusion weights. In [14], [15], the relationships between node topology and PCRLB are derived, and the optimal topology selection scheme by minimizing PCRLB is designed. According to these schemes, the tracking accuracy is improved by choosing some specific topologies. Mutual information (MI) is also proposed as a utility metric in [16], [17]. Therefore, nodes with maximal MI are selected to achieve high-precision tracking [16]. The trace of error covariance is also considered during the cluster selection in [18]. Inspired by Euclidean distance, literature [19] uses Mahalanobis distance to evaluate the information utility of nodes, in spite of this method is only suitable for distance measurement. In the aforementioned literature, node selection algorithms are all designed based on a single criterion. In engineering, however, it may be biased due to focus on only one criterion. What's more, in some situation, the nodes selected by different criteria are inconsistent. So, it's necessary to comprehensively consider the criteria to select nodes better.

Therefore, studying multi-objective optimization problem (MOP) is of great importance. Recently, the MOP has also been introduced into node selection to consider multiple criteria simultaneously. For example, Cao *et al.* formulate a MOP for the sensor selection problem where the tradeoff between performance gap and energy budget is established [20]. Yang *et al.* [21] also put forward a MOP strategy for sensor selection in nonlinear scenario, where the sparsity-promoting penalty factor is added into the objective. Considering the correlated noise caused by the common reference sensor, a MOP is proposed in [22]. However, the weight sum method used in [22] commonly encounters difficulties in determining the weight or unifying the dimension, especially when it comes to the non-convex model. In contrast, multi-objective optimization solves those difficulties and is capable of determining vast pareto front for choice. For the reasons above, multi-objective optimization is proved to be suitable for node selection.

In recent years, as the application background of target tracking has become more and more complex, node selection is no longer limited to the ideal environment. So, problems of node selection when there are uncertainties in sensor networks also have attracted much attention. Cao N *et al.* study the sensor selection problem in uncertain WSNs where the uncertainty is caused by occlusions, i.e., the sensors maybe unable to sense the target when blocked by some obstacles [20]. In [23], considering the mixture gaussian noise, a sensor selection method is developed. By comprehensively considering two positioning performance criteria for node selection, this method makes up for the gaps in existing research. The problem of measurement origin uncertainty is also studied in [24]. The existing researches are mostly based on WSNs, and few researches on USNs consider the uncertainties in nodes. These underwater node selection algorithms mostly don't take the influence of ocean currents on the position of underwater sensor nodes into consideration. Starting from this, our article will also study the node selection algorithm on target tracking based on USNs under position floating.

To overcome the limitations above, in this paper, a node selection algorithm based on multi-objective optimization under position floating is proposed. The main contributions of our proposed algorithm can be summarized as follows:

1) The particle filter under position floating (PF-PF) is put forward which takes position floating into consideration and introduces the addition floating noise into filter.
2) Both Fisher information matrix (FIM) and mutual information (MI) under position floating are derived with the help of PF-PF.
3) The node selection problem is constructed into a multi-objective optimization problem. The number of nodes, the FIM and MI under position floating are set as the objective function, which avoids the problem of inconsistent selection based on single criterion under position floating.

The rest of the paper proceeds as follows. In section II, the target tracking problem is formulated and the PF-PF is also put forward. As the criteria, both FIM and MI under position floating are derived in section III. In section IV, a node selection algorithm based on multi-objective optimization is designed which is solved by both NSGA-II and TOPSIS. In section V, simulation results are presented to verify the effectiveness of our algorithm. Finally, conclusions of this paper are drawn in section VI.

II. PROBLEM FORMULATION

A. STATE MODEL

We consider that the target can be modeled as a maneuvering point which moves at constant velocity (CV) in an underwater three-dimensional space. The target state is given by [25]:

$$X_k = F_{k-1}X_{k-1} + G_{k-1}\omega_{k-1} \tag{1}$$

where the target state at time k is given by $X_k = [x, \dot{x}, y, \dot{y}, z, \dot{z}]^T$, $u = [x, y, z]^T$ and $v = [\dot{x}, \dot{y}, \dot{z}]^T$ are the

position vector and velocity vector in x, y, and z coordinate, respectively; F_{k-1} is the state transition matrix; G_{k-1} is the process noise matrix; the process noise ω_{k-1} is assumed to be Gaussian with zero mean and covariance matrix Q_{k-1}. In CV model, the F_{k-1} and G_{k-1} are given as follows:

$$F_{k-1} = \begin{bmatrix} 1 & T & 0 & 0 & 0 & 0 \\ 0 & 1 & 0 & 0 & 0 & 0 \\ 0 & 0 & 1 & T & 0 & 0 \\ 0 & 0 & 0 & 1 & 0 & 0 \\ 0 & 0 & 0 & 0 & 1 & T \\ 0 & 0 & 0 & 0 & 0 & 1 \end{bmatrix} \tag{2}$$

$$G_{k-1} = \begin{bmatrix} \frac{T^3}{3} & \frac{T^2}{2} & 0 & 0 & 0 & 0 \\ \frac{T^2}{2} & T & 0 & 0 & 0 & 0 \\ 0 & 0 & \frac{T^3}{3} & \frac{T^2}{2} & 0 & 0 \\ 0 & 0 & \frac{T^2}{2} & T & 0 & 0 \\ 0 & 0 & 0 & 0 & \frac{T^3}{3} & \frac{T^2}{2} \\ 0 & 0 & 0 & 0 & \frac{T^2}{2} & T \end{bmatrix} \tag{3}$$

where T is the sampling interval.

B. MEASUREMENT MODEL

We assume that there are M underwater sensor nodes placed in USNs. When the tracking target is detected, the nodes will transmit sonic pulse and obtain the measurements by using time-of-arrival (TOA) [14]. The measurement of the nth node at time k is:

$$Z_k^n = h_k^n(X_k) + v_k^n = \|u - s_n\| + v_k^n \tag{4}$$

where $u = [x, y, z]^T$ and $s_n = [x_n, y_n, z_n]^T$ $(n = 1, 2, \cdots M)$ are the real position of the target and the nth node; v_k^n is the measurement noise of sensor n which is assumed to be Gaussian white noise which satisfies $v_k^n \sim N\left(0, r_m^2\right)$.

C. FLOATING NOISE CAUSED BY POSITION FLOATING

As discussed earlier, due to ocean current near the coast, underwater sensor nodes will float and produce changes in position which are assumed to be $\Delta s_n = [\Delta x_n, \Delta y_n, \Delta z_n]^T$ $(n = 1, 2, \cdots M)$. According to the knowledge of hydrodynamics and related literature [25], [26], the float of nodes is not an irregular process. It changes periodically, forming a similar sine curve. However, without the node location algorithm [27], [28] to correct the real position, usually, we can only know the estimate position of the nodes $\hat{s}_n = \left[\hat{x}_n, \hat{y}_n, \hat{z}_n\right]^T$, which satisfies:

$$\hat{s}_n = s_n + \Delta s_n \tag{5}$$

There are two approaches to handle the position floating above mentioned [29]. The first one appends the predicted node state vectors to the target state vector with the help of existing position prediction model. However, the computational complexity of this approach will increase which may not be suitable for tracking under high real-time requirement. Considering the requirement of real-time, we selected the second approach where the idea of Taylor series expansion is used. Through the Taylor expansion around $\hat{s}_n$, (4) can be rewritten as:

$$\begin{aligned} Z_k^n &= \|u - s_n\| + v_k^n \\ &= \left\|u - \hat{s}_n + \Delta s_n\right\| + v_k^n \\ &\approx \left\|u - \hat{s}_n\right\| + \rho_{u,\hat{s}_n}^T \Delta s_n + v_k^n \\ &= \left\|u - \hat{s}_n\right\| + v_{f,k}^n + v_k^n \\ &= \left\|u - \hat{s}_n\right\| + \bar{v}_k^n \end{aligned} \tag{6}$$

$$\bar{v}_k^n = v_{f,k}^n + v_k^n = \rho_{u,\hat{s}_n}^T \Delta s_n + v_k^n \tag{7}$$

where $\rho_{u,s_n}^T = \left(u - \hat{s}_n\right)^T / \left\|u - \hat{s}_n\right\|$. Compare (4) and (6), we can find, after considering the position floating of nodes, a new variable $\rho_{u,\hat{s}_n}^T \Delta s_n$ will produced which called floating noise $v_{f,k}^n$ in this paper. Based on the simulation result in [26] and the knowledge of Bartlett's test, this noise could be easily tested to be white noise. Besides, according to the central limit theorem (CLT), the noise caused by environmental disturbance can also be regarded as Gaussian noise.

So, in order to facilitate the analysis of the problem and the design of algorithm, we assume Δs_n to be Gaussian white noise vector which satisfies $N\left(0, r_f^2\right)$. Then, the mean and variance of floating noise $v_{f,k}^n$ could respectively be calculated as:

$$E\left[v_{f,k}^n\right] = \rho_{u,\hat{s}_n}^T E\left(\Delta s_n\right) = 0 \tag{8}$$

$$\begin{aligned} r_f^2 &= E\left[\left(v_{f,k}^n\right)^2\right] \\ &= \text{power}\left(\rho_{u,\hat{s}_n}^T, 2\right) \cdot E\left[\text{power}\left(\Delta s_n, 2\right)\right] \end{aligned} \tag{9}$$

where power (A, B) means raise each element of A to the corresponding powers in B. Therefore, after calculation, $v_{f,k}^n$ will also be a Gaussian white noise with variance satisfies (9). Hence, after converting Δs_n into $v_{f,k}^n$, the variance of $\bar{v}_k^n$ will be:

$$r_{total}^2 = r_f^2 + r_m^2 \tag{10}$$

D. PARTICLE FILTER UNDER POSITION FLOATING

Particle filter (PF) can solve nonlinear and non-Gaussian problems of underwater target tracking [30], [31]. Considering position floating, we put forward an improved PF which called particle filter under position floating (PF-PF). Unlike PF, PF-PF takes the situation when nodes floated due to ocean currents into consideration, so the estimate position of the nodes and floating noise are applied.

In PF-PF, the *probability density function* (pdf) of the measurement likelihood which obtained by the

nth node at time k is:

$$p\left(Z_k^n|x_k^i\right) = \frac{\exp\left[-\frac{1}{2}(\Delta Z)^T\left(r_{total}^2\right)^{-1}(\Delta Z)\right]}{\sqrt{2\pi r_{total}^2}} \tag{11}$$

where $\Delta Z = Z_k^n - \left\|x_k^i - \hat{s}_n\right\|$; x_k^i is the ith particle at time k. The measurement likelihood over all M nodes will be:

$$p\left(Z_k|x_k^i\right) = \prod_{n=1}^{M} p\left(Z_k^n|x_k^i\right) \tag{12}$$

where $Z_k = \left[Z_k^1, Z_k^2, \cdots, Z_k^M\right]^T$. Adopting $p\left(x_k|x_{k-1}\right)$ as the proposal distribution, the importance weights of particles would be:

$$\omega_k^i = \omega_{k-1}^i p\left(Z_k|x_k^i\right) \tag{13}$$

The detailed PF-PF is listed as Algorithm 1. From (11), (12) and (13), it can be seen that measurements under position floating does have effects on the result of estimation.

Algorithm 1 Particle Filter Under Position Floating

1: Set $k = 0$, draw initial particle x_0^i from the prior of target state $p\left(x_0\right)$;
2: **for** $k = 1, 2, 3, \ldots$ **do**
3: Propagating particles by (1);
4: Update the importance weights by (11), (12), and (13);
5: Normalize weights $\omega_k^i = \omega_k^i / \sum_{i=1}^N \omega_k^i$;
6: Resampling $\left\{x_k^i, N^{-1}\right\} \sim \left\{x_k^i, \omega_k^i\right\}$;
7: Estimate target state $\hat{X}_k = \sum_{i=1}^N \omega_k^i x_k^i$;
8: **end for**

III. NODE SELECTION CRITERIA UNDER POSITION FLOATING

A. FIM UNDER POSITION FLOATING

As the inverse of the posterior Cramer low bound, FIM provides the theoretical limit on the mean square error (MSE) of target state estimation during tracking. The FIM on the MSE is represented as:

$$E\left[\hat{X}_k - X_k\right]\left[\hat{X}_k - X_k\right]^T \geq J_k^{-1} \tag{14}$$

where $\hat{X}_k$ is the estimate of X_k and J_k is the FIM at kth time. Assuming that J_{k-1} has already been known, J_k can be calculated as:

$$J_k = D_{k-1}^{22} - D_{k-1}^{22}\left(J_{k-1} + D_{k-1}^{11}\right)^{-1} D_{k-1}^{12} \tag{15}$$

where:

$$D_{k-1}^{11} = E\left[-\nabla_{X_{k-1}}\nabla_{X_{k-1}}^T lnp\left(x_k|x_{k-1}\right)\right] \tag{16}$$

$$D_{k-1}^{12} = E\left[-\nabla_{X_k}\nabla_{X_{k-1}}^T lnp\left(x_k|x_{k-1}\right)\right] \tag{17}$$

$$D_{k-1}^{21} = E\left[-\nabla_{X_{k-1}}\nabla_{X_k}^T lnp\left(x_k|x_{k-1}\right)\right] \tag{18}$$

$$D_{k-1}^{22} = E\left[-\nabla_{X_k}\nabla_{X_k}^T lnp\left(x_k|x_{k-1}\right)\right] + E\left[-\nabla_{X_k}\nabla_{X_k}^T lnp\left(x_k|x_{k-1}\right)\right] \tag{19}$$

where ∇_{X_k} is the first-order partial derivation operator about X_k. (16), (17), (18) and the first part of (19) are depend on the motion model of the target, while the second part of (19) shows the dependency of FIM on measurements, which also has a relationship with the position floating of the nodes. In CV model, these equations could be further calculated as [31]:

$$D_{k-1}^{11} = F_{k-1}^T Q_{k-1}^{-1} F_{k-1} \tag{20}$$

$$D_{k-1}^{12} = -F_{k-1}^T Q_{k-1}^{-1} \tag{21}$$

$$D_{k-1}^{21} = -Q_{k-1}^{-1} F_{k-1}^T \tag{22}$$

$$D_{k-1}^{22} = Q_{k-1}^{-1} + \Lambda_k \tag{23}$$

$$\Lambda_k = E\left\{-\nabla_{X_k}\nabla_{X_k}{}^T \ln p\left(Z_k|X_k\right)\right\} \tag{24}$$

Equation (24) presents the part where the FIM corresponding to the priori information. According to [31], (24) can be further approximated as:

$$\Lambda_k \approx \left(H_k^n\right)^T\left(r_{total}^2\right)^{-1}\left(H_k^n\right) \tag{25}$$

where H_k^n is the Jacobian matrix for the nth nodes at time k, which can be calculated as:

$$H_k^n = \begin{bmatrix} \frac{\hat{x} - \hat{x}_n}{\left\|\hat{u} - \hat{s}_n\right\|} & 0 & \frac{\hat{y} - \hat{y}_n}{\left\|\hat{u} - \hat{s}_n\right\|} & 0 & \frac{\hat{z} - \hat{z}_n}{\left\|\hat{u} - \hat{s}_n\right\|} & 0 \end{bmatrix} \tag{26}$$

where $\hat{u} = \left[\hat{x}, \hat{y}, \hat{z}\right]^T$ is the estimate position of the target, which can be obtained from PF-PF. Substituting (25), (26) into (24), Λ_k can be given by:

$$\Lambda_k = \begin{bmatrix} \gamma_k^{11} & 0 & \gamma_k^{13} & 0 & \gamma_k^{15} & 0 \\ 0 & 0 & 0 & 0 & 0 & 0 \\ \gamma_k^{31} & 0 & \gamma_k^{33} & 0 & \gamma_k^{35} & 0 \\ 0 & 0 & 0 & 0 & 0 & 0 \\ \gamma_k^{51} & 0 & \gamma_k^{53} & 0 & \gamma_k^{55} & 0 \\ 0 & 0 & 0 & 0 & 0 & 0 \end{bmatrix} \tag{27}$$

where:

$$\gamma_k^{11} = \frac{1}{N}\sum_{i=1}^{N} \frac{\left(\hat{x} - \hat{x}_n\right)^2}{r_{total}^2\left\|\hat{u} - \hat{s}_n\right\|^2} \tag{28}$$

$$\gamma_k^{33} = \frac{1}{N}\sum_{i=1}^{N} \frac{\left(\hat{y} - \hat{y}_n\right)^2}{r_{total}^2\left\|\hat{u} - \hat{s}_n\right\|^2} \tag{29}$$

$$\gamma_k^{55} = \frac{1}{N}\sum_{i=1}^{N} \frac{\left(\hat{z} - \hat{z}_n\right)^2}{r_{total}^2\left\|\hat{u} - \hat{s}_n\right\|^2} \tag{30}$$

$$\gamma_k^{13} = \gamma_k^{31} = \frac{1}{N}\sum_{i=1}^{N} \frac{\left(\hat{x} - \hat{x}_n\right)\left(\hat{y} - \hat{y}_n\right)}{r_{total}^2\left\|\hat{u} - \hat{s}_n\right\|^2} \tag{31}$$

$$\gamma_k^{15} = \gamma_k^{51} = \frac{1}{N}\sum_{i=1}^{N} \frac{\left(\hat{x} - \hat{x}_n\right)\left(\hat{z} - \hat{z}_n\right)}{r_{total}^2\left\|\hat{u} - \hat{s}_n\right\|^2} \tag{32}$$

$$\gamma_k^{35} = \gamma_k^{53} = \frac{1}{N}\sum_{i=1}^{N}\frac{(\hat{y}-\hat{y}_n)(\hat{z}-\hat{z}_n)}{r_{total}^2\left\|\hat{u}-\hat{s}_n\right\|^2} \tag{33}$$

where N is the particle number used in PF-PF. After introducing PF-PF, in this paper, there is no need to obtain the measurement of the target Z_{k+1} at time $k+1$. Once $\hat{X}_k$ is known, the FIM of each node under position floating at time $k+1$ will able to be calculated. Hence, FIM can be used to select nodes for target tracking. Meanwhile, FIM is calculated by PF-PF which does not need to be obtained through multiple Monte Carlo like [32]. So, with less calculation, it would be more suitable for the underwater sensor nodes with limited computing power. The detailed way to calculate FIM is listed as Algorithm 2.

Algorithm 2 FIM Under Position Floating at Time k

while $i \le M$ **do**
  Estimate Target State $\hat{x}_k$ by Algorithm 1;
  Compute the Λ_k by (27);
  $D_{k-1}^{22} = Q_{k-1}^{-1} + \Lambda_k$;
  $D_{k-1}^{11} = F_{k-1}^T Q_{k-1}^{-1} F_{k-1}$;
  $D_{k-1}^{12} = -F_{k-1}^T Q_{k-1}^{-1}$;
  $D_{k-1}^{21} = -Q_{k-1}^{-1} F_{k-1}^T$;
  $J_{k,i} = D_{k-1}^{22} - D_{k-1}^{22}\left(J_{k-1,i} + D_{k-1}^{11}\right) D_{k-1}^{12}$;
  The FIM of the ith node at time k is $J_{k,i}$;
end while

Figure 1 shows the trends of FIM under different floating noises while keep the original measurement noise unchanged. As we can see from Figure 1, FIM finally levels off after the increasement. Besides, the growth of FIM is reduced with the increase of r_f^2. The result shows that FIM is related to the floating noise, so the selected nodes can be evaluated by FIM.

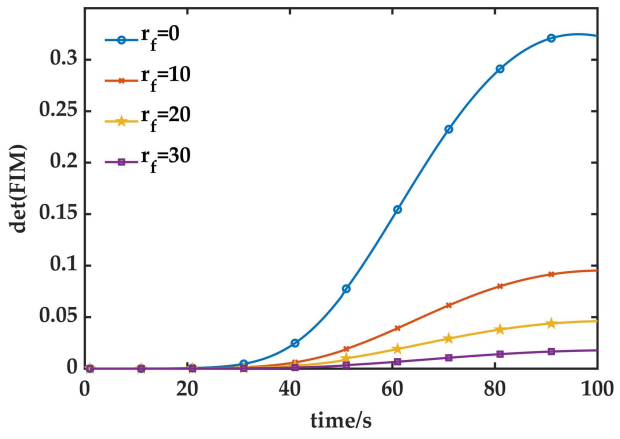

FIGURE 1. Relationship between FIM and floating noise.

B. MI UNDER POSITION FLOATING

MI provides the relativity between two variables [33]. At time k, the mutual information between the measurement Z_k^n of the nth node and the target state X_k can be calculated as:

$$MI\left(X_k, Z_k^n\right) = H\left(Z_k^n\right) - H\left(Z_k^n|X_k\right) \tag{34}$$

where:

$$\begin{aligned} H\left(Z_k^n\right) &= -\int p\left(Z_k^n\right)\log p\left(Z_k^n\right) dZ_k^n \\ &= -\int_{Z_k^n}\left\{\int_{X_k} p\left(Z_k^n|X_k\right)p\left(X_k\right)dx\right\} \\ &\quad\cdot\left\{\log\left[\int_{X_k} p\left(Z_k^n|X_k\right)p\left(X_k\right)dx\right]\right\} dZ_k^n \end{aligned} \tag{35}$$

$$H\left(Z_k^n|X_k\right) = -\int p\left(X_k\right)\left\{\int p\left(Z_k^n|X_k\right)\log p\left(Z_k^n|X_k\right) dX_k\right\} \tag{36}$$

where $MI(\cdot)$ represents the mutual information; $H\left(Z_k^n\right)$ represents the entropy of the measurement Z_k^n; $H\left(Z_k^n|X_k\right)$ represents the conditional entropy of the measurement Z_k^n given the target state X_k.

We also use the idea of PF-PF to calculate the MI under position floating. Considering there is no closed-form solution to $p\left(Z_k^n\right)$, similarly, the idea of posterior particle is used to obtain the approximated solution. So $p\left(Z_k^n\right)$ could be calculated as:

$$p\left(Z_k^n\right) \approx \frac{1}{N}\sum_{i=1}^{N} p\left(Z_k^n|x_{k|k-1}^i\right) \tag{37}$$

where $x_{k|k-1}^i$ is the ith predicted particle and its importance weight is $1/N$. Substituting (37) into (35) and (36), $H\left(Z_k^n\right)$ and $H\left(Z_k^n|X_k\right)$ can be rewritten as:

$$\begin{aligned} H\left(Z_k^n\right) &= -\sum_{Z_k^n}\left\{\frac{1}{N}\sum_{i=1}^{N} p\left(Z_k^n|x_{k|k-1}^i\right)\right\} \\ &\quad\cdot\left\{\log\frac{1}{N}\sum_{i=1}^{N} p\left(Z_k^n|x_{k|k-1}^i\right)\right\} \end{aligned} \tag{38}$$

$$H\left(Z_k^n|X_k\right) = -\sum_{Z_k^n}\left\{\frac{1}{N}\sum_{i=1}^{N} p\left(Z_k^n|x_{k|k-1}^i\right)\log p\left(Z_k^n|x_{k|k-1}^i\right)\right\} \tag{39}$$

So far, we have obtained the MI under position floating. It should be noted that the calculation of MI is only based on the final predicted particle, which means once the information of particle are obtained, we can use (34) to estimate the MI under position floating without the measurement at time $k+1$. Therefore, the computational complexity is also not large by this way. The detailed calculation method of MI is listed as Algorithm 3.

Figure 2 shows the relationship between MI and floating noise. As we can see from this figure, there are obvious differences between each MI under different floating noises.

Algorithm 3 MI Under Position Floating at Time k

```
while i ≤ M do
    if n = N then
        Sample x_k^n (Z_k^n | X_k) by Algorithm 1;
    end if
    Compute H(Z_k^i) by (38);
    Compute H(Z_k^i | X_k) by (39);
    MI(X_k, Z_k^i) = H(Z_k^i) − H(Z_k^i | X_k);
    The MI of the ith node at time k is MI(X_k, Z_k^i);
end while
```

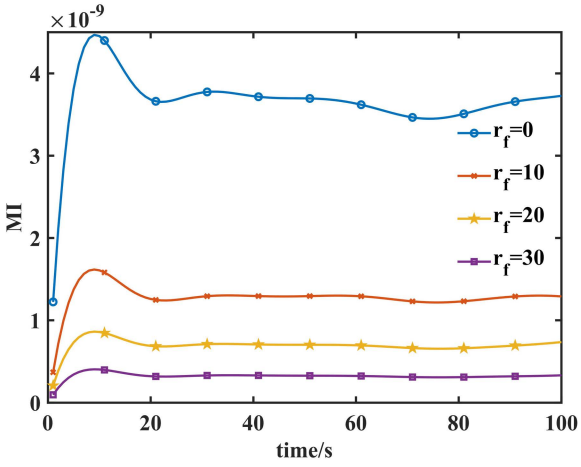

FIGURE 2. Relationship between MI and floating noise.

Besides, the range of MI also reduces with the increase of r_f^2. The results above prove that the floating noise also affects MI.

IV. NODE SELECTION ALGORITHM BASED ON MULTI-OBJECTIVE OPTIMIZATION

A. NODE SELECTION PROBLEM BASED ON MULTI-OBJECTIVE

According to the analysis above, both FIM and MI would be affected by floating noise. So, we can use FIM or MI under position floating to select nodes. Considering the difference in selection results between FIM-based and MI-based under position floating, a novel node selection algorithm based on multi-objective optimization is proposed after consider these two criteria comprehensively.

First, both FIM and MI can quantitatively measure the information value that each underwater sensor nodes can provide. The larger the FIM or MI, the more information the node can provide. Therefore, in order to obtain enough information for tracking, at each sampling time, the total FIM and MI of the selected nodes should be as large as possible, which could be given by:

$$\max f_1(\omega) = \sum_{i=1}^{M} \omega_i det(J_i) \tag{40}$$

$$\max f_2(\omega) = \sum_{i=1}^{M} \omega_i MI_i \tag{41}$$

where ω_i is a Boolean variable which means whether the node is selected. When $\omega_i = 1$, the node i will be selected; otherwise, it will be ignored.

Considering the limitation on the battery of underwater sensor nodes, excess nodes participating in tracking will consume lots of energy and affect the lifetime of the USNs. Therefore, the number of nodes is also be set as an objective function. In ideal, the number of selected nodes should be as few as possible, which could be given by:

$$\min f_3(\omega) = \sum_{i=1}^{M} \omega_i \tag{42}$$

After transforming (42) into a maximization problem and eliminating the dimensional differences through normalization, we transform the node selection problem into a multi-objective optimization problem:

$$\max\ F(\omega) = \{f_1(\omega), f_2(\omega), f_3(\omega)\}, \omega \in \{0,1\}^M \tag{43}$$

$$\begin{cases} f_1(\omega) = \dfrac{\sum_{i=1}^{M} \omega_i \det(J_i)}{\sum_{i=1}^{M} \det(J_i)} \\ f_2(\omega) = \dfrac{\sum_{i=1}^{M} \omega_i \mathrm{MI}_i}{\sum_{i=1}^{M} \mathrm{MI}_i} \\ f_3(\omega) = \dfrac{M - \sum_{i=1}^{M} \omega_i}{M} \end{cases} \tag{44}$$

Theoretically, the more nodes involved into tracking, the better tracking effect could be obtained; however, more energy would also be consumed. Therefore, these three optimization objectives have co-constraints, traditional weighted techniques to transform the multi-objectives problem into a single-objective problem is difficult to solve this problem. In this paper, we use multi-objective optimization and decision-making algorithms to find the optimal solution of the problem above.

B. NODE SELECTION OPTIMIZATION ALGORITHM BASED ON NSGA-II

For such multi-objective optimization problems:

$$\min\ y = F(x) = (f_1(x), f_2(x), \cdots f_n(x)) \tag{45}$$

where $x \in R^n$ is the vector of decision variables, $y \in R^n$ is the objective vector. In MOP, there exists no single global optimal solution, but a set which consists of multiple non-inferior optimal solutions, namely, pareto optimal solution set. The goal of multi-objective optimization and decision-making algorithm is to find such pareto optimal solution set through optimization algorithm, and select the optimal solution through decision-making technology.

Considering computational efficiency, in this paper, non-dominated sorting genetic algorithm II (NSGA-II) is used to get the pareto optimal solution set of the node selection problem under position floating. With the fast nondominated sorting approach, diversity preservation and main loop, NSGA-II has been widely used, the full algorithm can be seen from [34].

After using more optimized nondominated sorting and excellence mechanism, the computational complexity of NSGA-II significantly surpasses its predecessor NSGA. Besides, it is quite different from the priori methods like weight sum method and epsilon-constraint method which turn the MOP into the single one, NSGA-II avoids high redundancy caused by weight selection and the poor robustness due to inconsistent dimensions.

C. NODE SELECTION DECISION TECHNOLOGY BASED ON TOPSIS

After obtaining the pareto optimal solution set through NSGA-II, finding the final node selection scheme from these pareto set becomes a decision-making problem. For node selection during tracking, it is necessary to balance the tracking performance and the lifetime of USNs. Taking the finiteness of energy into account, therefore, we tend to reduce the number of selected nodes as much as possible under the premise of ensuring a certain tracking performance.

Finally, we use the Technique for Order of Preference by Similarity to Ideal Solution (TOPSIS) [35] to make the final decision. TOPSIS takes both the positive ideal solution and the negative ideal solution into consideration at the same time. With the help of Euclidean distance, TOPSIS select the optimal solution which is closest to the positive ideal solution and farthest from the negative ideal solution. The TOPSIS used in this paper is:

Step1: For each objective, construct decision matrix R^k, $k = 1 \cdots K$, and normalize it with the help of (46):

$$r_{ij} = \frac{x_{ij}}{\sqrt{\sum_{j=1}^{n} x_{ij}^2}} \quad i = 1 \cdots m, \quad j = 1 \cdots n \tag{46}$$

where x_{ij} represents the objective j corresponding to the ith solution; r_{ij} is the normalized value of x_{ij}.

Step2: Introduce weights to construct a weighted decision matrix:

$$v_{ij} = r_{ij} \times \omega_j \tag{47}$$

where ω_j is the weight of the objective j; v_{ij} is the weight of r_{ij}.

Step3: For each objective, determine the positive ideal and negative ideal solutions V^{k+} and V^{k-}, respectively.

Step4: Calculate the separation measure from V^{k+} and V^{k-}, S_i^+ and S_i^-, respectively:

$$S_i^+ = \sqrt{\sum_{j=1}^{n} \left(v_{ij} - \max\left(v_j\right)\right)}, \quad i = 1 \cdots m \tag{48}$$

$$S_i^- = \sqrt{\sum_{j=1}^{n} \left(v_{ij} - \min\left(v_j\right)\right)}, \quad i = 1 \cdots m \tag{49}$$

Step5: Calculate the performance score for each solution:

$$P_i = \frac{S_i^-}{S_i^+ + S_i^-} \tag{50}$$

where $0 \leq P_i \leq 1$. So, the final node selection scheme is the scheme corresponding to the solution with the highest performance score:

$$S_{k+1}^{opt} = \arg\max P_i \tag{51}$$

The full pseudo codes for our algorithm are listed as Algorithm 4.

Algorithm 4 Our Node Selection Algorithm Based on Multi-Objective Optimization

```
if k = 0 then
    for i = 1, 2, ..., N do
        Particle initialization by the first step of Algorithm 1;
    end for
end if
for k = 1, 2, ... do
    Draw particles by Algorithm 1;
    if n = N then
        Calculate all the MI of nodes under position floating at time k by Algorithm 3;
    end if
    Estimate target state X̂_k by Algorithm 1;
    Calculate all the FIM of nodes under position floating at time k by Algorithm 2;
    Obtain the pareto optimal solution set through NSGA-II;
    Obtain the final node selection scheme through TOPSIS by (46)-(51)
end for
```

D. COMPUTATIONAL COMPLEXITY ANALYZE

The node selection algorithm based on multi-objective optization proposed in this paper uses PF-PF to calculate FIM and MI. According to [36], the computational complexity is $O(n)$ when systematic resampling is used. The computational complexity of calculating FIM and MI for M nodes are $O(M)$ and $O(Mn)$, respectively.

For NSGA-II, the basic operations and their worst-case complexities are as follows: fast nondominated sorting is $O\left(m(2N)^2\right)$, diversity preservation is $O\left(m\,(2N)\log(2N)\right)$, main loop is $O\left(2N\log(2N)\right)$. The overall complexity of the NSGA-II is $O\left(mN^2\right)$ which is smaller than $O\left(mN^3\right)$ by using NSGA [34].

In TOPSIS, Step1 need to construct decision matrix which computational complexity is $O(mK)$; times product operations are performed in Step2, so its complexity is $O(mK)$; Step4 is $O(2mK)$. The overall complexity of the TOPSIS is $O(mK)$.

In summary, the computational complexity of the node selection algorithm proposed in this paper is $O\left(Mn + mN^2 + mK\right)$, where m is the number of objectives, M is the number of underwater sensor nodes, n is the number of particles and N is the population size of NSGA-II.

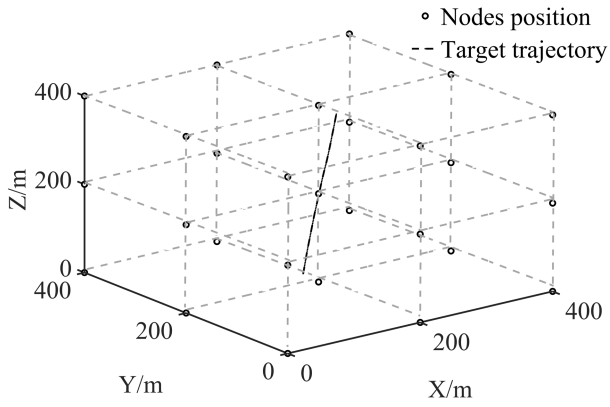

FIGURE 3. Simulation scenario.

V. SIMULATION AND ANALYSIS

In order to verify the effectiveness of the proposed algorithm, in this section, some simulations are conducted to analyze the influence of the weight in TOPSIS, position floating noise and node selection strategy on the algorithm.

Simulations are set up as follows. The underwater sensor nodes are evenly deployed over a test region of size $400m \times 400m \times 400m$, as shown in Figure 3, and the minimum distance between nodes is $200m$. Other parameters are set as follows: the initial state of the target $X_0 = [100, 2, 100, 2, 100, 2]$, the initial estimate state of the target $\hat{X}_0 = [105, 2, 95, 2, 100, 2]$, the standard deviation of measurement noise $r_m = 10$, the sampling time $T = 1s$, the particle number $N = 1000$ and the simulation runs $\gamma = 50$.

To indicate the accuracy of target tracking after node selection, we adopt root mean square error (RMSE) defined as follows, to measure the tracking performance:

$$RMSE\,(k) = \sqrt{\sum_{i=1}^{\gamma} \frac{X_{k,i} - \hat{X}_{k,i}^2}{\gamma}} \tag{52}$$

where $X_{k,i}$ and $\hat{X}_{k,i}$ are the real and the estimated positions of the target at time k, respectively, in the ith simulation.

A. SIMULATION FOR PARETO OPTIMAL SOLUTION SET BASED ON NSGA-II

In this subsection, we take the result at the $100th$ sampling interval as an example to show the optimization of NSGA-II. For NSGA-II, the population size is chosen as $P = 100$. In Figure 4, the pareto optimal solution set obtained using NSGA-II is presented.

According to Figure 4, NSGA-II can find relatively uniform non-dominated solutions. Even when the number of nodes is same, different node combinations can still be determined.

B. SIMULATION OF THE INFLUENCE OF THE WEIGHT IN TOPSIS ON NODE SELECTION

In this subsection, simulations are presented to study the influence of the weight in TOPSIS on the algorithm proposed.

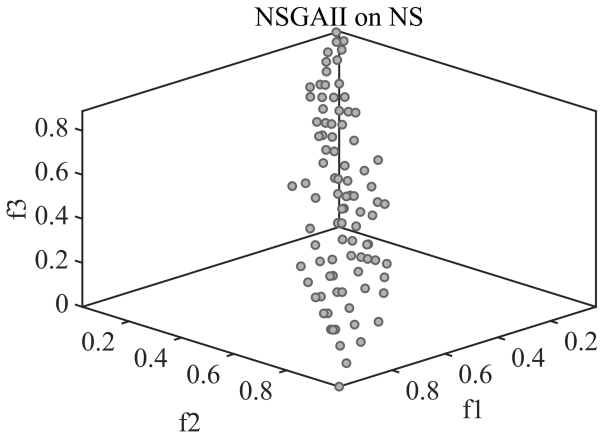

FIGURE 4. Pareto optimal solution set based on NSGA-II.

TABLE 1. Average RMSE and SN with different weights.

Weights of TOPSIS	Average RMSE/m	Average SN
$[0.4, 0.45, 0.15]$	6.154	4.37
$[0.4, 0.4, 0.2]$	6.133	5.66
$[0.35, 0.35, 0.3]$	6.118	8.93

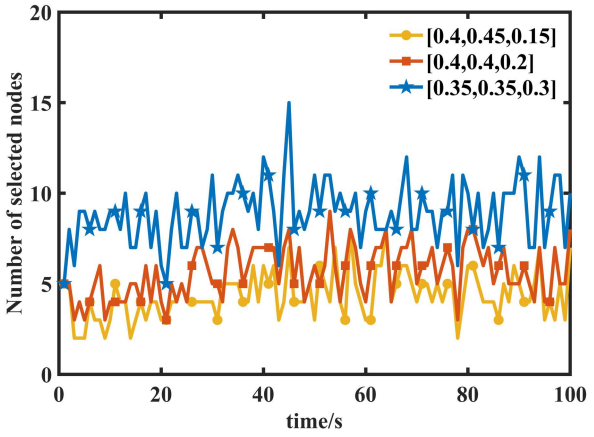

FIGURE 5. Number of selected nodes by TOPSIS with different weights.

Three different weights are selected for simulation. The number of selected nodes with different weights are shown in Figure 5 and the RMSE with different weights are also shown in Figure 6. Table 1 shows the detailed average RMSE and the average number of selected nodes (SN).

According to Table 1, when $\omega = [0.4, 0.4, 0.2]$, the average number of selected nodes is 5.66 which is 36.6% less than the 8.93 when $\omega = [0.35, 0.35, 0.3]$. In comparison, the average RMSE only increased by 0.245%. It shows that there is no need to select excessive underwater sensor nodes to achieve less promotion on tracking performance. Illustrated from Figure 5, when $\omega = [0.4, 0.45, 0.15]$, only two or three nodes will be selected out frequently. According to [4] and Figure 6, in 3D scenario, few nodes will have an impact on tracking performance. So, the weight of TOPSIS is selected as $[0.4, 0.4, 0.2]$ in the further simulation, which also proves that the weight really has an impact on node selection.

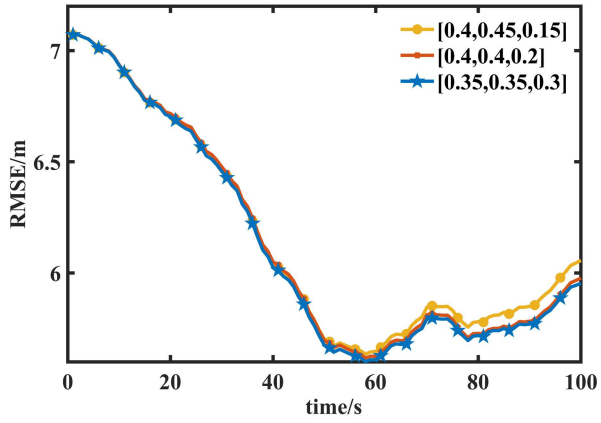

FIGURE 6. RMSE by TOPSIS with different weights.

TABLE 2. Average RMSE and improvement with different floating noise.

r_f	Average RMSE/m			Improvement
	OU	IS	PFU	
10	6.146	6.134	6.151	0.08%
20	6.191	6.174	6.226	0.57%
30	6.206	6.178	6.281	1.21%

C. SIMULATION OF THE INFLUENCE OF POSITION FLOATING NOISE ON NODE SELECTION

In this subsection, simulations are presented to study the influence of position floating noise on the algorithm proposed. By changing the standard deviation of floating noise r_f, we analyze the performance of algorithm. Besides our algorithm, algorithm under ideal situation which is based on true location of nodes and the algorithm which the position floating is unconsidered are simulated to compare. The results of RMSE under different floating noise are plotted in Figure 7 to Figure 10, respectively. As a summary, Table 2 shows the detailed average RMSE under different floating noise and the improvement compared our algorithm with the algorithm when the position floating is unconsidered.

According to Table 2, with the increase of node floating noise, the tracking accuracy of the two non-ideal algorithms has decreased. As we can see from Figure 7, when r_f is small, the difference of RMSE of these two algorithms is only 0.005; as r_f increases, like Figure 8 and Figure 9, the advantage of the algorithm proposed is revealed: no matter what r_f is taken, compared with the other algorithm, the algorithm our proposed has the tracking effect closer to the ideal situation. All the analyses show that the proposed algorithm can effectively select nodes in the scene of node position floating. It can also overcome the influence of position floating to a large extent and has good robustness.

D. SIMULATION OF THE INFLUENCE OF NODE SELECTION STRATEGY ON NODE SELECTION

In this subsection, simulations are presented to study the tracking performance of node selection strategy on the algorithm proposed. Besides our algorithm (OU) proposed in this paper, the algorithm based on nearest neighbors (NN) [10],

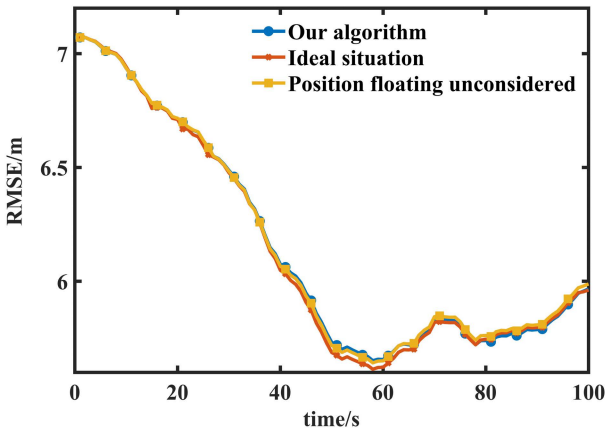

FIGURE 7. RMSE with $r_f = 10$.

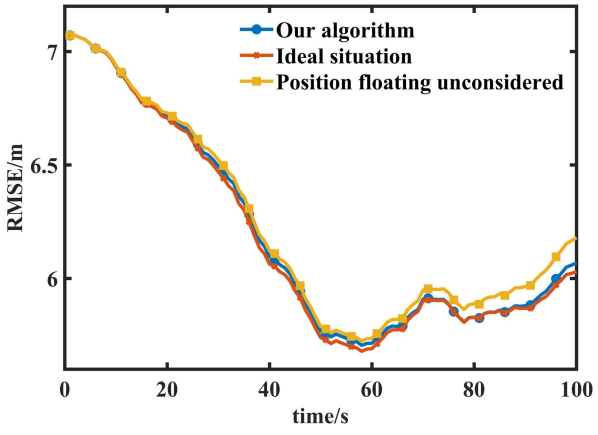

FIGURE 8. RMSE with $r_f = 20$.

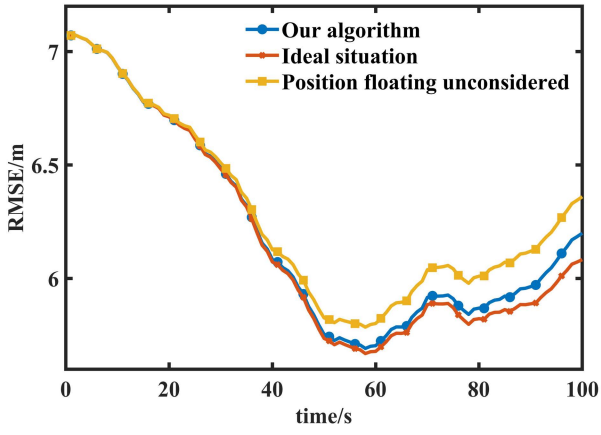

FIGURE 9. RMSE with $r_f = 30$.

the algorithm based on minimum number (MN) [37], the algorithm based on FIM [13] and the algorithm based on MI [16] are also simulated for comparison. The standard deviation of floating noise $r_f = 30$, all the other parameters are same as those set in the previous. The results are plotted in Figure 11. Table 3 shows the detailed average RMSE and the average number of selected nodes (SN) under different node selection strategies.

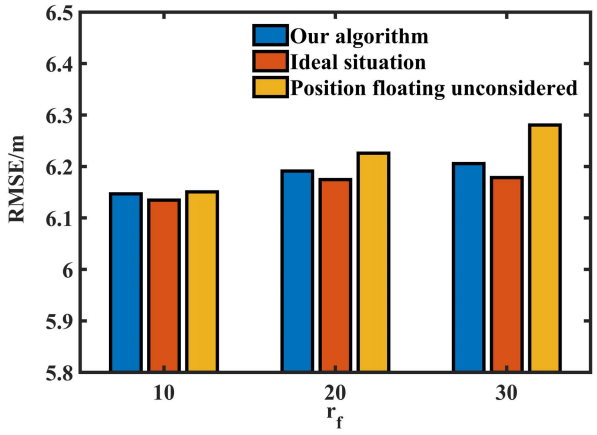

FIGURE 10. Average RMSE when r_f changes.

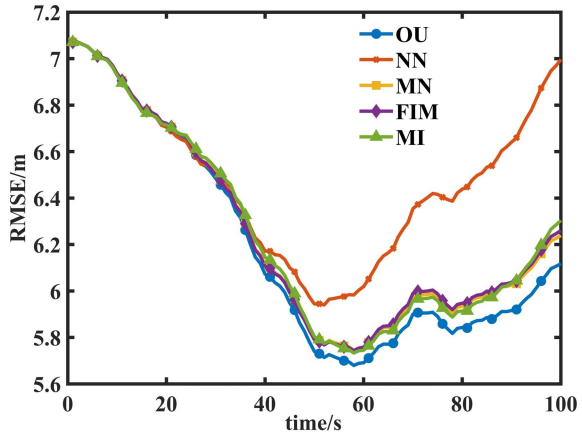

FIGURE 11. RMSE under different node selection strategies.

TABLE 3. Average RMSE and SN under different node selection strategies.

Node selection strategy	Average RMSE/m	Average SN
OU	6.188	5.66
NN	6.478	1.00
MN	6.242	7.42
FIM	6.246	5.66
MI	6.246	5.66

According to Table 3, with the minimum number of nodes, NN achieves the worst tracking performance. Besides, the others have similar tracking performance as we can see in Figure 11. Owing to the large threshold, MN will select more nodes than others and bound to consume more energy. Due to comprehensive consideration of various criteria, the node selection algorithm based on multi-objective optimization proposed in this paper can make a trade-off between FIM, MI and the number of nodes, thus it achieves more stable and better tracking performance while saving in terms of the number of selected nodes.

VI. CONCLUSION

In this paper, a node selection algorithm based on multi-objective optimization under position floating is proposed. Firstly, through Taylor series expansion, the position floating error is converted into a kind of floating noise. Then, after putting forward a particle filter under position floating, both FIM and MI are derived as the criteria for node selection. Finally, both NSGA-II and TOPSIS are employed to find the optimal node selection scheme which avoid the problem of inconsistent node selection of single-criteria algorithm. To verify the effectiveness of our scheme, simulations are carried out and the results show that the tracking performance can be improved by considering position floating. In the future works, more attention will be paid to the node selection algorithm based on the actual situation and the real data with the help of neural network.

REFERENCES

[1] H. Ghafoor and Y. Noh, "An overview of next-generation underwater target detection and tracking: An integrated underwater architecture," *IEEE Access*, vol. 7, pp. 98841–98853, 2019.
[2] V. A. Reddy and G. L. Stüber, "Wi-buoy: An energy-efficient wireless buoy network for real-time high-rate marine data acquisition," *IEEE Access*, vol. 9, pp. 130586–130600, 2021.
[3] J. Luo, Y. Han, and L. Fan, "Underwater acoustic target tracking: A review," *Sensors*, vol. 18, no. 2, p. 112, Jan. 2018.
[4] G. Isbitiren and O. B. Akan, "Three-dimensional underwater target tracking with acoustic sensor networks," *IEEE Trans. Veh. Technol.*, vol. 60, no. 8, pp. 3897–3906, Oct. 2011.
[5] H. Luo, K. Wu, R. Ruby, Y. Liang, Z. Guo, and L. M. Ni, "Software-defined architectures and technologies for underwater wireless sensor networks: A survey," *IEEE Commun. Surveys Tuts.*, vol. 20, no. 4, pp. 2855–2888, 4th Quart., 2018.
[6] I. F. Akyildiz, D. Pompili, and T. Melodia, "Underwater acoustic sensor networks: Research challenges," *Ad Hoc Netw.*, vol. 3, no. 3, pp. 257–279, Mar. 2005.
[7] D. Zhang, M. Liu, S. Zhang, and Q. Zhang, "Non-myopic energy allocation for target tracking in energy harvesting UWSNs," *IEEE Sensors J.*, vol. 19, no. 10, pp. 3772–3783, May 2019.
[8] L. Jing, C. He, J. Huang, and Z. Ding, "Energy management and power allocation for underwater acoustic sensor network," *IEEE Sensors J.*, vol. 17, no. 19, pp. 6451–6462, Oct. 2017.
[9] J. Feng, H. Zhao, and B. Lian, "Efficient and adaptive node selection for target tracking in wireless sensor network," *J. Sensors*, vol. 2016, pp. 1–9, Jan. 2016.
[10] Y. Huang, W. Liang, H. Yu, and Y. Xiao, "Target tracking based on a distributed particle filter in underwater sensor networks," *Wireless Commun. Mobile Comput.*, vol. 8, no. 8, pp. 1023–1033, 2008.
[11] Q. Zhang, C. Zhang, M. Liu, and S. Zhang, "Local node selection for target tracking based on underwater wireless sensor networks," *Int. J. Syst. Sci.*, vol. 46, no. 16, pp. 2918–2927, Nov. 2015.
[12] M. Poostpasand and R. Javidan, "An adaptive target tracking method for 3D underwater wireless sensor networks," *J. Wireless Netw.*, vol. 24, no. 8, pp. 2797–2810, Nov. 2018.
[13] D. Zhang, M.-Q. Liu, S.-L. Zhang, Z. Fan, and Q.-F. Zhang, "Mutual-information based weighted fusion for target tracking in underwater wireless sensor networks," *Frontiers Inf. Technol. Electron. Eng.*, vol. 19, no. 4, pp. 544–556, Apr. 2018.
[14] Q. Zhang, M. Liu, S. Zhang, and H. Chen, "Node topology effect on target tracking based on underwater wireless sensor networks," in *Proc. 17th Int. Conf. Inf. Fusion (FUSION)*, Salamanca, Spain, Jul. 2014, pp. 1–8.
[15] Q. Zhang, M. Liu, and S. Zhang, "Node topology effect on target tracking based on UWSNs using quantized measurements," *IEEE Trans. Cybern.*, vol. 45, no. 10, pp. 2323–2335, Oct. 2015.
[16] N. Adurthi, P. Singla, and M. Majji, "Mutual information based sensor tasking with applications to space situational awareness," *J. Guid., Control, Dyn.*, vol. 43, no. 4, pp. 767–789, Apr. 2020.
[17] Y. Zhang and L. Gao, "Sensor-networked underwater target tracking based on grubbs criterion and improved particle filter algorithm," *IEEE Access*, vol. 7, pp. 142894–142906, 2019.
[18] X. Han, M. Liu, S. Zhang, and Q. Zhang, "A multi-node cooperative bearing-only target passive tracking algorithm via UWSNs," *IEEE Sensors J.*, vol. 19, no. 22, pp. 10609–10623, Nov. 2019.

[19] A. A. Soderlund and M. Kumar, "Optimization of multitarget tracking within a sensor network via information-guided clustering," *J. Guid., Control, Dyn.*, vol. 42, no. 2, pp. 317–334, Feb. 2019.
[20] N. Cao, S. Choi, E. Masazade, and P. K. Varshney, "Sensor selection for target tracking in wireless sensor networks with uncertainty," *IEEE Trans. Signal Process.*, vol. 64, no. 20, pp. 98841–98853, Oct. 2016.
[21] X. Yang and R. Niu, "Adaptive sensor selection for nonlinear tracking via sparsity-promoting approaches," *IEEE Trans. Aerosp. Electron. Syst.*, vol. 54, no. 4, pp. 1966–1982, Aug. 2018.
[22] Z. Li, Y. Zhao, N. Cheng, B. Hao, J. Shi, R. Zhang, and X. Shen, "Multiobjective optimization based sensor selection for TDOA tracking in wireless sensor network," *IEEE Trans. Veh. Technol.*, vol. 68, no. 12, pp. 12360–12374, Dec. 2019.
[23] Q. Yan and J. Chen, "Sensor selection method based on multi-objective optimal optimization for mixture Gaussian noise," *J. Electron. Inf. Technol.*, vol. 43, no. 2, pp. 341–348, 2021, doi: 10.11999/JEIT191031.
[24] D. Zhang, M. Liu, and S. Zhang, "Node selection for target tracking in UWSNs under measurement origin uncertainty," in *Proc. 35th Chin. Control Conf. (CCC)*, Chengdu, China, Jul. 2016, pp. 5154–5159.
[25] H. Chen, M. Liu, and S. Zhang, "Energy-efficient localization and target tracking via underwater mobile sensor networks," *Frontiers Inf. Technol. Electron. Eng.*, vol. 19, no. 8, pp. 999–1012, 2018, doi: 10.11999/JEIT191031.
[26] S. Kim and Y. Yoo, "High-precision and practical localization using seawater movement pattern and filters in underwater wireless networks," in *Proc. IEEE 16th Int. Conf. Comput. Sci. Eng.*, Sydney, NSW, Australia, Dec. 2013, pp. 374–381.
[27] W. Zhang, G. Han, X. Wang, M. Guizani, K. Fan, and L. Shu, "A node location algorithm based on node movement prediction in underwater acoustic sensor networks," *IEEE Trans. Veh. Technol.*, vol. 69, no. 3, pp. 3166–3178, Mar. 2020.
[28] P. Jiang, J. Liu, B. Ruan, L. Jiang, and F. Wu, "A new node deployment and location dispatch algorithm for underwater sensor networks," *Sensors*, vol. 16, no. 1, p. 82, Jan. 2016.
[29] K. Punithakumar, T. Kirubarajan, and M. Hernandez, "Multisensor deployment using PCRLBS, incorporating sensor deployment and motion uncertainties," *IEEE Trans. Aerosp. Electron. Syst.*, vol. 42, no. 4, pp. 1474–1485, Oct. 2006.
[30] H. Zhang, W. Liu, Z. Zhang, W. Lu, and J. Xie, "Joint target assignment and power allocation in multiple distributed MIMO radar networks," *IEEE Syst. J.*, vol. 15, no. 1, pp. 694–704, Mar. 2021.
[31] X. Zhang, P. Willett, and Y. Bar-Shalom, "Dynamic Cramér–Rao bound for target tracking in clutter," *IEEE Trans. Aerosp. Electron. Syst.*, vol. 41, no. 4, pp. 1154–1167, Oct. 2005.
[32] Z. Duan, V. P. Jilkov, and X. R. Li, "State estimation with quantized measurements: Approximate MMSE approach," in *Proc. 11th Int. Conf. Inf. Fusion*, Cologne, Germany, Jun./Jul. 2008, pp. 1–6.
[33] Y. Zhang and L. Gao, "Target tracking with underwater sensor networks based on Grubbs criterion and improved particle filter algorithm," *J. Electron. Inf. Technol.*, vol. 41, no. 10, pp. 2294–2301, 2019, doi: 10.11999/JEIT190079.
[34] K. Deb, A. Pratap, S. Agarwal, and T. Meyarivan, "A fast and elitist multiobjective genetic algorithm: NSGA-II," *IEEE Trans. Evol. Comput.*, vol. 6, no. 2, pp. 182–197, Aug. 2002.
[35] H.-S. Shih, H.-J. Shyur, and E. S. Lee, "An extension of TOPSIS for group decision making," *Math. Comput. Model.*, vol. 45, nos. 7–8, pp. 801–813, 2007.
[36] M. Bolić, P. M. Djurić, and S. Hong, "Resampling algorithms for particle filters: A computational complexity perspective," *EURASIP J. Adv. Signal Process.*, vol. 2004, no. 15, pp. 1–11, Dec. 2004.
[37] S. P. Chepuri and G. Leus, "Sparsity-promoting sensor selection for nonlinear measurement models," *IEEE Trans. Signal Process.*, vol. 63, no. 3, pp. 684–698, Feb. 2015.

SHENGKAI TIAN received the B.S. degree from the Tongda College, Nanjing University of Posts & Telecommunications. He is currently pursuing the M.S. degree with the Jiangsu University of Science and Technology. His research interest includes underwater target tracking.

ZHENKAI ZHANG received the Ph.D. degree in signal and information processing from the Nanjing University of Aeronautics and Astronautics. He is currently an Associate Professor with the Jiangsu University of Science and Technology. His current research interests include radar signal processing, and target localization and tracking.